Numerical Demonstration of the Soliton Self-Frequency Shift Process Beyond 8 μm in a Tellurite-Chalcogenide Fiber Cascaded Structure

Yiwei Hou, Qi Wu, Fei Liu, Aoke Yan, Francois Ouellette, and Jianfeng Li, *Senior Member, IEEE*

***Abstract*—We investigate theoretically the mid-infrared (MIR) Raman soliton self-frequency shift (SSFS) process in the TeO_2-BaF_2-Y_2O_3 (TBY) fiber and $AsSe_2$-As_2S_5 fiber. The numerical analysis of the SSFS process in the TBY fiber is performed, revealing the impacts of the pumping wavelength and fiber core diameter on the SSFS effect. A new quantity measuring the frequency shift ability of a Raman shifter fiber is derived to interpret the complex relation between the frequency shift amount and the fiber parameter observed in simulations. Further, we propose some general ways to optimize the wavelength extension, conversion efficiency, pulse duration, and spectrum cleanliness for all Raman soliton lasers. For the first time, we propose the idea of coupling the tellurite fiber with chalcogenide fiber to further enhance the SSFS effect in MIR. With experimentally achievable high-power seed pulses at 1.9 μm and 2.8 μm, we demonstrated wavelength conversion from 1.9 to 7.5 μm and 2.8 to 8.1 μm through the SSFS process by cascading the TBY fiber with a $AsSe_2$-As_2S_5 fiber in suitable coupling parameters. Our work could offer meaningful guidance to optimize the Raman soliton lasers and enlighten a feasible way to extend the SSFS process to a longer wavelength range.**

***Index Terms*—Soliton self-frequency shift, mid-infrared, tellurite fiber, chalcogenide fiber.**

I. Introduction

FIBER-based ultrashort lasers in the mid-infrared region (MIR) are of great significance for a wide range of applications such as spectroscopy [1], gas sensing [2], eye-safe LIDAR [3], and attosecond pulse generation [4]. As an important nonlinear wavelength conversion mechanism in optical fibers, the soliton self-frequency shift (SSFS) effect [5] has been one of the most promising ways to build fiber-based widely tunable Raman soliton lasers. Most recently, the SSFS process in various Raman shifter fibers such as thulium-doped [6], [7], germanium-doped [8]–[10], fluoride [11], [12], tellurite [13]–[15], and chalcogenide [16]–[18] fibers has been studied and utilized to build tunable laser sources.

Limited by the position of the zero-dispersion wavelength (ZDW) of optical fibers, the pumping wavelength of these Raman shifter fibers in MIR is usually $\sim$2 μm or $\sim$2.8 μm, which has been achieved by mode-locked thulium-doped fiber lasers [19], [20] and holmium- [21] or erbium-doped fiber lasers [22], respectively. By pumping at $\sim$2 μm, the GeO_2-doped silica-based fiber almost reaches 3 μm [9] through the SSFS effect. However, due to the high transmission loss of the silica-based materials beyond 3 μm, it is hard to achieve further wavelength extension through the SSFS process in these fibers. Owing to the low photon energy, soft glass fibers such as chalcogenide, fluoride, and tellurite fibers offer low fiber loss in the spectrum range beyond 3 μm [23], thus allowing the SSFS process in a longer wavelength range. The MIR SSFS process in fluoride fibers has been demonstrated intensively. For example, Duval *et al.* [11] achieved a 2.8-3.6 μm tunable ultrashort laser source with watt-level output using a ZBLAN fiber as the Raman shifter fiber. Tang *et al.* [12] built a widely tunable femtosecond laser source with an indium fluoride (InF_3) fiber covering the 2-4.3 μm spectrum region, which has been the widest SSFS process achieved in experiment up to now. However, due to the low nonlinearity, the achievement of wide tunability in fluoride fibers requires seed pulses with ultra-high power and ultra-short duration. Compared with fluoride fibers, tellurite fibers possess the merits of a much higher nonlinear coefficient and higher Raman contribution in MIR. This feature greatly enhances the SSFS effect, especially with a relatively ordinary seed pulse. Koptev *et al.* [13] achieved a widely tunable ultrashort laser source covering the 1.6-2.65 μm spectrum range in a TeO_2-WO_3-La_2O_3 (TWL) fiber with sub-125 pJ input energy. Most recently, Qin *et al.* [24] manufactured a fluorotellurite fiber based on TeO_2-BaF_2-Y_2O_3 (TBY) glass with high transparency in 0.5-5 μm. They subsequently demonstrated the generation of a 10-watt-level supercontinuum (SC) covering 947-3934 nm in that fiber [25]. Alternatively, this fiber is a promising candidate for the SSFS effect in MIR, owing to its high nonlinearity and

Manuscript received 31 March 2022; revised 26 June 2022; accepted 28 June 2022. Date of publication 11 July 2022; date of current version 18 July 2022. This work was supported in part by the National Natural Science Foundation of China under Grants U20A20210 and 62005040, in part by the Fundamental Research Funds for the Central Universities under Grants ZYGX2019Z012 and ZYGX2020KYQD003, in part by the Science and Technology Project of Sichuan Province under Grant 21YYJC2977, in part by Sichuan Province Science and Technology Support Program under Grant 2019YFH0091, and in part by the National College Student Innovation and Entrepreneurship Training Program under Grant 202110614077. *(Yiwei Hou and Qi Wu contributed equally to this work.) (Corresponding author: Jianfeng Li.)*

Yiwei Hou, Qi Wu, Fei Liu, Aoke Yan, and Jianfeng Li are with the State Key Laboratory of Electronic Thin Films and Integrated Devices, School of Optoelectronic Science and Engineering, University of Electronic Science and Technology of China, Chengdu 610054, China (e-mail: 1207713124@qq.com; 625339383@qq.com; feiliu_ly@126.com; liz327160303@163.com; lijianfeng@uestc.edu.cn).

Francois Ouellette is with the College of Information Science and Engineering, Chengdu University, Chengdu 130012, China (e-mail: fouellette58@yahoo.ca).

Digital Object Identifier 10.1109/JPHOT.2022.3187862

wide anomalous dispersion region. Using a 0.5 m-long 2.7-μm-core TBY fiber as the nonlinear medium, Li *et al.* [15] achieved a tunable laser source covering the 2-2.8 μm spectrum range with a 200 pJ, 189 fs pump pulse. Though the manufactured TBY fiber provides various core diameters to adjust its dispersion and nonlinearity, current experiments in the regime of SSFS are rare and far from satisfactory. Despite the fluoride and tellurite fibers have successfully extended the SSFS process to a longer wavelength range, their performance would greatly worsen in the spectrum beyond 4.5 μm for the steeply increasing fiber loss. Another promising candidate is the chalcogenide fiber, which offers low fiber loss even in the spectrum beyond 5 μm [17]. It has the potential to achieve further wavelength extension. However, chalcogenide fibers with such characteristics and a SSFS regime usually demand a seed pulse source >4 μm, which has not been achieved yet. At present, the experimental demonstration of the SSFS process in chalcogenide fibers is below 2.7 μm [18]. Despite soft glass fibers can offer impressive SSFS performance in MIR, the conversion efficiency is not satisfactory, due to the generation of noise solitons and dispersive waves under high input power. If increasing the pump power is used as the way of improving the SSFS effect, the reduction of conversion efficiency is inevitable. At the same time, with the increase of soliton order, the energy portion of the first fundamental soliton would decrease and the spectrum would evolve into SC. In this case, the engineering of the nonlinearity and dispersion of a Raman shifter fiber could be a more promising way to further improve the SSFS performance.

In the earlies, the full mathematical description of the SSFS effect in optical fibers, the generalized nonlinear Schrödinger equation (GNLSE), has been established [26]–[29]. Later, the re-derived GNLSE in the frequency domain [30] and the correction to the GNLSE in the temporal domain [31], [32] have been introduced to consider the frequency-dependency of the nonlinear coefficient, which makes the numerical calculation more trustworthy. Though great achievements have been made in experiments, the proceedings in the field of theory have been slow in recent years. Most theoretical works were aimed at offering theoretical accordance with the experiments [6], [12], [15] or predicting the SSFS performance in some designed or newly manufactured Raman shifter fibers [14], [17]. However, there are many questions in experiments waiting to be answered in the theory. Researchers are concerned with the optimization of the wavelength extension, conversion efficiency, and pulse duration of Raman soliton source in experiments. Besides improving the pump power and compressing the pulse duration, the engineering of the nonlinearity and dispersion is also a feasible way to achieve better SSFS performance. Nevertheless, these issues have not been clarified by theoretical works. Although chalcogenide fiber is the most promising candidate for wavelength extension beyond 5 μm through the SSFS effect, current theoretical works [17], [40] only demonstrated it with unrealized seed pulse. There have been no theoretical works pointing a feasible path to utilize its enormous potential up to now.

In this paper, we study numerically the SSFS process in the TBY fiber and the possibility of cascading the TBY fiber with chalcogenide fiber to achieve the SSFS process in a longer wavelength range. The comparative study of the SSFS performance in the TBY fiber with two typical pumping wavelengths and different core diameters enlighten the way to optimize the wavelength extension, conversion efficiency, and pulse duration for all Raman soliton systems. A new quantity W_{fiber} is introduced to measure the frequency shift ability of a Raman shifter fiber in the aspect of the coordination of nonlinearity and dispersion. By cascading the TBY fiber with the $AsSe_2$-As_2S_5 fiber in suitable geometrical parameters, we demonstrate the possibility of the SSFS process covering 1.9-7.5 μm and 2.8-8.1 μm spectrum range using experimentally achievable seed pulses.

II. Dispersion, nonlinearity, and Loss Spectrum of the TBY Fiber

Fig. 1 shows the group velocity dispersion (GVD) parameter β_2, nonlinear coefficient γ, and fiber loss of the TBY fiber with a core diameter of 4 μm, 5 μm, 6 μm, and 7 μm. Fig. 1(c) shows the β_2-wavelength curves, which are calculated using the refractive index data in [25]. One could see that the TBY fiber with all the core diameters we choose works in the anomalous dispersion region in the whole 2-5 μm spectrum range, enabling a Raman soliton regime. The TBY fiber with other core diameters beyond the 4-7 μm range does not possess this characteristic [15], [32]. The ZDW of the TBY fiber with the core diameter of 4 μm, 5 μm, 6 μm, and 7 μm is located at 1.52 μm, 1.73 μm, 1.81 μm, and 1.83 μm, respectively. The calculated nonlinear coefficient γ of the TBY fiber as a function of the wavelength is shown in Fig. 1(b). The nonlinear refractive index was taken as $n_2 = 3.5 \times 10^{-19}$ m^{2}W^{-1} [15] in the calculation. We could see from this figure that the γ value decreases with the increase of the core diameter and wavelength. The TBY fiber possesses a large nonlinear coefficient in MIR, which is almost two-order higher than the silica-based [8], [9] and fluoride fibers [23], [39]. Fig. 1(c) shows the measured [25] and fitted fiber loss of the TBY fiber. In MIR, the TBY fiber possesses low fiber loss (<4.5 dB/m below 5 μm), which would greatly benefit the transmission of the Raman soliton pulse. For simplicity of numerical calculation, the fitted fiber loss spectrum is taken. These parameters calibrate our numerical calculation of the pulse propagation in the TBY fiber.

III. Numerical Modeling

The generalized nonlinear Schrödinger equation (GNLSE) derived from the temporal domain [27] was used to simulate the pulse propagation in optical fibers:

$$\frac{\partial A(z,T)}{\partial z} = -\frac{\alpha}{2}A(z,T) + \sum_{n\geq 1}\beta_n \frac{i^{n+1}}{n!}\frac{\partial^n}{\partial T^n}A(z,T) + i\gamma(1+i\tau_{shock}) \left(A(z,T)\int_{-\infty}^{+\infty} R(t')|A(T-t')|^2 dt'\right) \quad (1)$$

where $A(z,T)$ is the complex temporal profile, α is the fiber loss, β_n is the dispersion coefficient associated with the Taylor

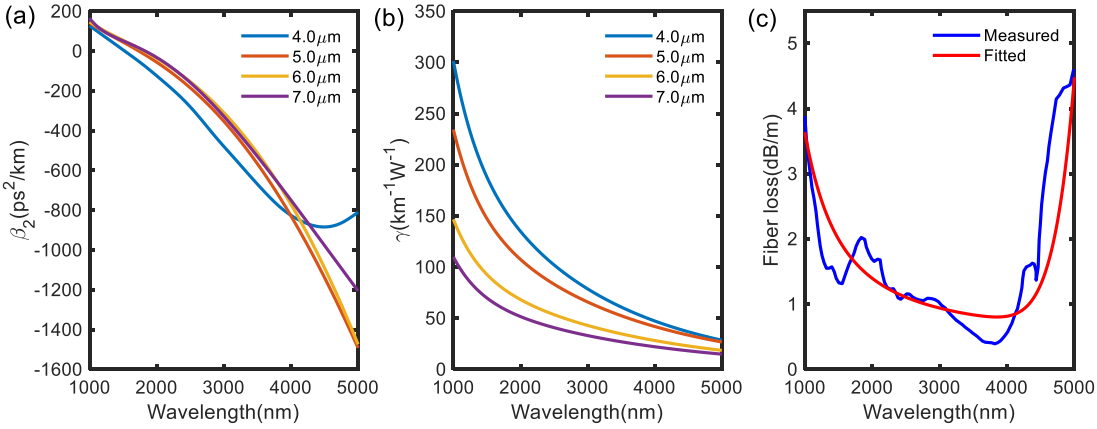

Fig. 1. Calculated (a) group velocity dispersion parameter and (b) nonlinear coefficient for TBY fibers ranging from 4 to 7 μm. (c) The measured and fitted loss spectrum of TBY fiber. Data source: [15], [25] and [32].

expansion of the propagation constant at the reference frequency, γ is the nonlinear coefficient, and τ_{shock} is the additional shock time. $R(t)$ is the Raman response function that includes both instantaneous electronic and delayed Raman contributions:

$$R(t) = (1 - f_R)\,\delta(t) + f_R h_R(t) \tag{2}$$

where f_R is the Raman contribution to the total nonlinear response and is 0.29 [17] for the TBY fiber. $h_R(t)$ is the delayed Raman response:

$$h_R(t) = \frac{\tau_1^2+\tau_2^2}{\tau_1+\tau_2^2}\exp\left(-\frac{t}{\tau_2}\right)\sin\left(\frac{t}{\tau_1}\right) \tag{3}$$

where $\tau_1 = 7.2$ fs, $\tau_2 = 59.3$ fs [15] for the TBY fiber.

The pump pulse was modeled as a hyperbolic secant field profile:

$$A(0,T) = \sqrt{P_0}\,\mathrm{sech}\,(T/T_0) \tag{4}$$

where P_0 is the pump peak power and T_0 is the characteristic pulse width related to the full width at half maximum (FWHM) duration

$$T_{FWHM} = 2\sqrt{\ln(2)}T_0 \tag{5}$$

The soliton order of the pump pulse was calculated as:

$$N^2 = \frac{\gamma P_0 T_0^2}{|\beta_2|} \tag{6}$$

When a high-order soliton breaks up into several fundamental solitons, the peak power and duration of the fundamental soliton follows the formula [34]:

$$\begin{cases} P_k = \frac{P_0(2N-2k+1)^2}{N^2} \\ T_k = \frac{T_0}{2N-2k+1} \end{cases} \tag{7}$$

where k is the number of the ejected soliton, P_k and T_k are the peak power and pulse duration of the kth ejected fundamental soliton, respectively.

The spilt-up Fourier method [34] was used to solve the GNLSE, in which the equation was divided into the linear and nonlinear part and solved in a subdivided distance of the whole fiber length. Since the spectrum we investigate is rather wide, the frequency-dependence of the parameters in GNLSE should be considered appropriately. The linear part in GNLSE, including the dispersion and loss term, was integrated in the frequency domain, which fully includes the frequency-dependence [35]. The nonlinear part was integrated in the temporal domain using a fourth-order Runge-Kutta method [36]. The frequency-dependence of the nonlinear coefficient was considered by introducing a correction to the mode effective area [31], [32]:

$$\tau_{shock} = \tau_0 + \left[\frac{1}{n_{\mathrm{eff}}(\omega)}\frac{dn_{\mathrm{eff}}(\omega)}{d\omega}\right] - \left[\frac{1}{A_{\mathrm{eff}}(\omega)}\frac{dA_{\mathrm{eff}}(\omega)}{d\omega}\right]_{\omega_0} \tag{8}$$

where $n_{eff}(\omega)$ is the guided mode effective index and $A_{eff}(\omega)$ is the mode effective area. The frequency-dependence of n_{eff} is typically very small compared to that of A_{eff} [32], so the second term in formula (8) can be neglected.

To ensure the accuracy of the numerical calculations, discretization points of 2^{16}, step size of 5 μm, and dispersion coefficients up to the 12^{th} order were taken.

IV. Numerical Analysis of the SSFS Process in the TBY Fiber

A. Impacts of the Pumping Wavelength

First, we have investigated the difference of the SSFS process in TBY fiber with pump wavelength at 1.96 μm and 2.8 μm. A 15 cm-long TBY fiber with a core diameter of 6 μm was used as the Raman shifter fiber. The sech^2 shape pump pulses with a pulse width of 100 fs at the full width at half maximum (FWHM) were launched into the fiber at 1.96 μm and 2.8 μm, respectively. The calculated output spectra using the two pumping schemes are shown in Fig. 2(a) and (b), respectively. The pump peak power is set to 1 kW, 5 kW, 10 kW, 20 kW, 30 kW, 50 kW, 80 kW, 100 kW, and 120 kW. The corresponding soliton order is 2.8, 6.2, 8.8, 12.4, 15.2, 19.6, 24.8, 30.3 at 1.96 μm, and 0.8, 1.8, 2.5, 3.5, 4.3, 5.6, 7.0, 7.9, 8.6 at 2.8 μm. With the same power and shape, the pump pulse at 1.96 μm has a higher soliton order than that at 2.8 μm, due to the higher γ and lower β_2 value at

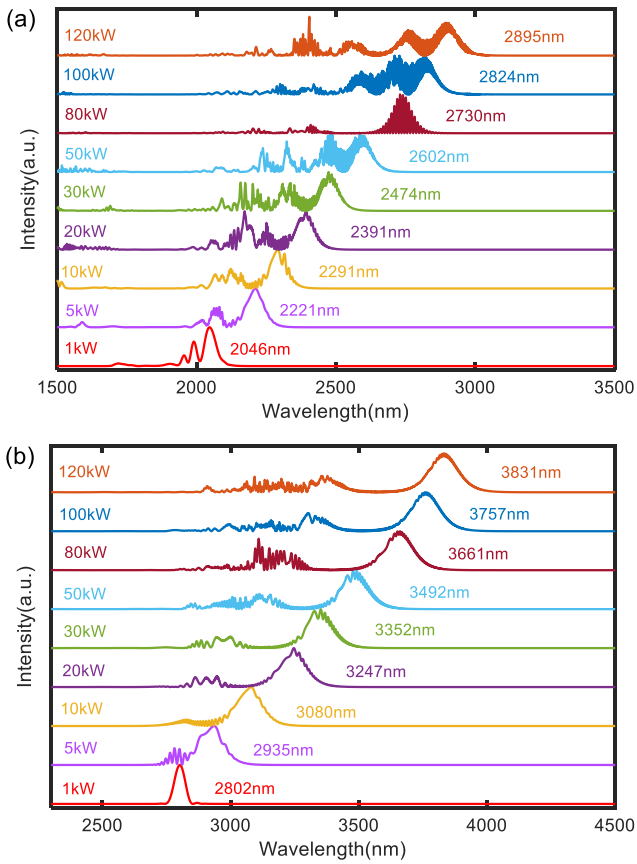

Fig. 2. Simulation results of the (a) spectra and (b) temporal profiles of the output pulses when pumping at 1.96 μm; (c) spectra and (d) temporal profiles of the output pulses when pumping at 2.8 μm.

1.96 μm. The new frequency component (i.e., Raman soliton) was generated through the effect of intrapulse Raman scattering [34]. When the peak power is 1 kW, the pump pulse at 1.96 μm breaks up while at 2.8 μm it still maintains the initial shape, for the soliton order is less than a unit. With the pump power increasing, the Raman solitons shift to a longer wavelength due to the SSFS effect [15]. By changing the pump peak power from 1 kW to 120 kW, the most shifted Raman soliton could cover the spectrum range of 1960-2895 nm when pumping at 1.96 μm, and 2800-3831 nm when pumping at 2.8 μm. With the same pump power, it is clear that the TBY fiber with pump pulse at 2.8 μm produces Raman solitons with a longer wavelength. As a consequence of a higher soliton order, more solitons were generated in the spectrum with the pump pulse at 1.96 μm. It should be noted that as the pump power increases, the spectrum would gradually evolve into SC. This process is obvious with the 1.96-μm-pump and is still obscure with the 2.8-μm-pump, for its lower soliton order slows this process.

To further explore the impacts of the pumping wavelength on the Raman soliton sources, the most red-shifted soliton in the temporal domain was filtered and analyzed. Fig. 3(a) displays the frequency conversion of the most shifted soliton as a function of the pump peak power. It is clear that with the same pump power and shape, a larger frequency shift can be obtained using the 1.96-μm-pump. This is in good agreement with the conclusion drawn in [37], [38] that the "higher nonlinearity, lower dispersion" combination could bring a larger frequency conversion. However, as displayed in Fig. 2, the cleanliness of the output spectrum using the 1.96-μm-pump is worse than that obtained using the 2.8-μm-pump as the consequence of a higher soliton order. The conversion efficiency of the two pumping schemes at different pump power is displayed in Fig. 3(b). One could see that at the same pump power, lower conversion efficiency was achieved with a 1.96-μm-pump, which is also resulted from the higher soliton order at 1.96 μm. At the 120-kW pump power, the conversion efficiency of the most red-shifted soliton with the 1.96-μm-pump and 2.8-μm-pump is 23.1% and 38.7%, respectively. Fig. 3(c) displays the pulse width of the two pumping schemes at different pump peak power. When the pump peak power is 1 kW, the output soliton with the 2.8-μm-pump has a pulse width of 649 fs, which is much wider than the pulse obtained using 1.96 μm. This is caused by the lower nonlinearity at 2.8 μm, which does not support the soliton fission with such low power. When the pump power increases to 5 kW, the pulse width decreases steeply to 127 fs due to the soliton fission process. As the pump peak power further increases, the pulse width of each pumping scheme increases gradually. It is obvious that with the same pump power, the pulse width of the output solitons when pumping at 1.96 μm is lower than those pumping at 2.8 μm. This is because the pump pulses at 1.96 μm have a higher soliton order, resulting in solitons with a shorter pulse duration in the fission process, as indicated in formula (7). Besides, at 1.96 μm, the TBY fiber has a higher nonlinear coefficient and lower GVD value, leading to a weaker temporal compression effect.

The evolution of the Raman solitons with pump peak power of 120 kW is shown in Fig. 4. Fig. 4(a) and (b) display the central wavelength and pulse duration of the most red-shifted soliton versus the propagation distance. The most red-shifted soliton was sampled every 1.5 cm through the propagation distance. Around 81% and 76% wavelength conversion were achieved in the first 1.5 cm when the pump wavelength is set at 1.96 μm and 2.8 μm, respectively. This indicates that a centimeter-scale length is enough for the TBY fiber as a nonlinear medium for the SSFS effect. Moreover, a shorter fiber length is needed for the SSFS effect when the pump wavelength is set at 1.96 μm, due to the higher nonlinearity there. At 1.5 cm, the duration and energy of the most red-shifted soliton obtained using a 1.96-μm and 2.8-μm pump are 87 fs, 3.2 nJ and 97 fs, 5.5 nJ, respectively. The soliton pulse possesses a shorter pulse width than the pump pulse, due to the process of soliton fission. The soliton pulse obtained using the 1.96-μm-pump has a higher soliton order. As a consequence, it has a shorter duration and lowers energy as the pump pulse breaks up in the initial stage, which is indicated in the formula (7). On passing the distance $>$1.5 cm, the anomalous dispersion is getting larger. The soliton pulse experienced a continuous temporal broadening and energy loss to maintain a unit soliton number. However, this process is only accompanied by a minor wavelength conversion, manifesting the inefficiency of the following propagation distance. The increasing dispersion and fiber loss are the main obstacles

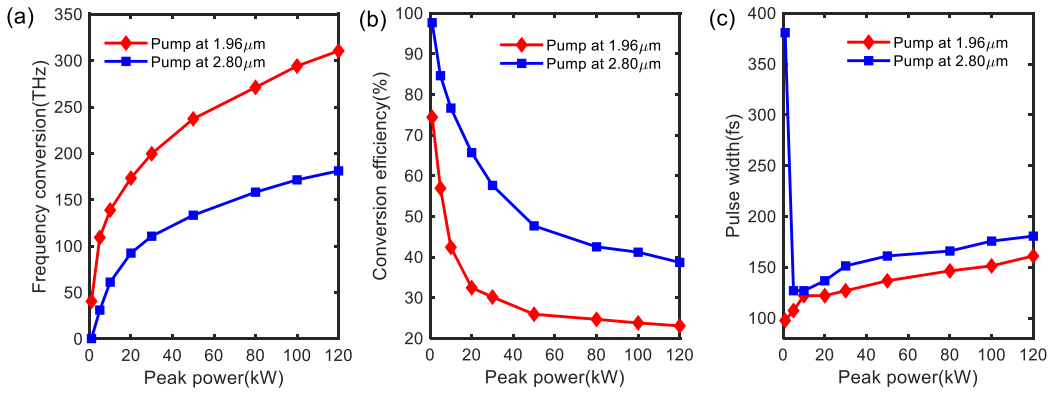

Fig. 3. Comparison of the (a) frequency conversion, (b) conversion efficiency, and (c) pulse width of the two pumping schemes.

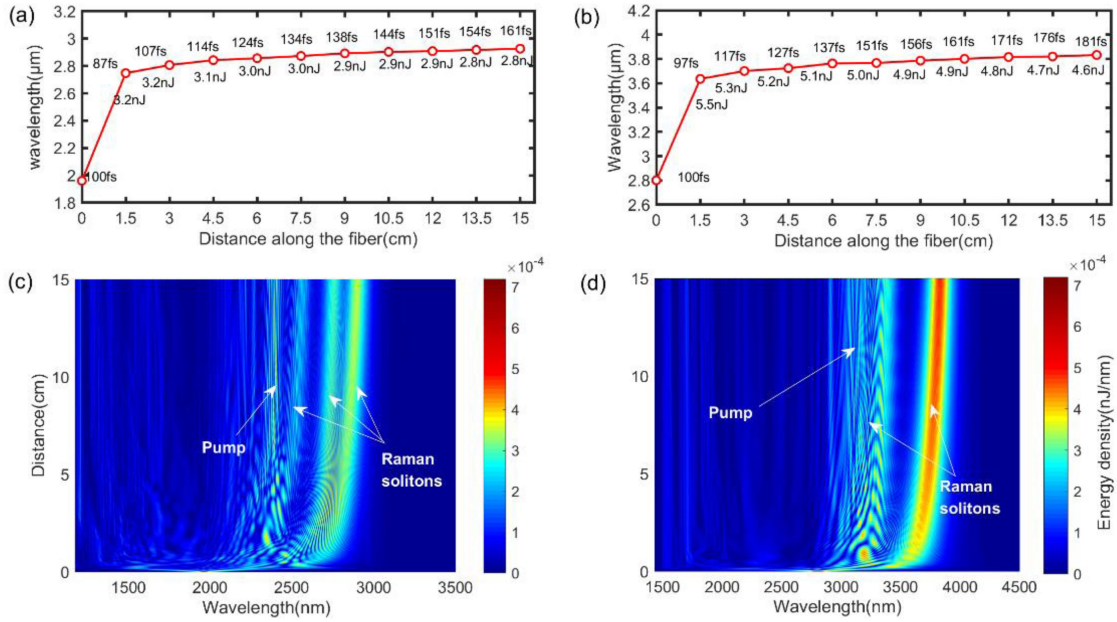

Fig. 4. The calculated wavelength, pulse width, and energy of the most red-shifted soliton versus propagation distance when (a) pumping at 1.96 μm and (b) pumping at 2.8 μm. The spectrum evolution versus propagation distance when (c) pumping at 1.96 μm and (d) pumping at 2.8 μm.

for the longer wavelength extension of solitons. The TBY fiber has a smaller anomalous dispersion and larger nonlinearity at 1.96 μm, meaning a stronger temporal compression effect. This characteristic results in a slower temporal broadening process when the pump wavelength is set at 1.96 μm. At 15 cm, the most red-shifted soliton obtained using a 1.96-μm-pump has a pulse duration of 161 fs, much shorter than the 181 fs outcome using the 2.8-μm-pump. Fig. 4(c) and (d) display the calculated spectrum evolution versus propagation distance with the two pumping schemes. The fission of the high-order soliton occurred in the initial stage with the generation of fundamental solitons and dispersive waves in the normal dispersion region. One could see clearly that there are three solitons and two solitons in the spectrum with 1.96-μm and 2.8-μm-pump, respectively. Then the fundamental solitons subsequently experienced a continuous redshift through the propagation distance. The spectral evolution in the two cases is qualitatively similar. The most red-shifted soliton with the 2.8 μm pumping scheme shifted much further and accumulated higher energy than the other ones. While with pump pulse at 1.96 μm, the three solitons were quite close in the spectrum and had an equivalent energy density. The principle behind this phenomenon is that the pump pulse at 1.96 μm has a higher soliton order, similar to the case discussed in the preceding content.

B. Impacts of the Fiber Core Diameter

The dispersion and nonlinear coefficient of a Raman shifter fiber are also crucial factors influencing the SSFS process. Changing the core diameter of the TBY fiber can easily adjust the nonlinearity and dispersion [25]. Therefore, it is meaningful to study the impacts of fiber core diameter on the SSFS process for further optimization. Table I shows the β_2 and γ values of TBY fiber with core diameters of 4 μm, 5 μm, 6 μm and 7 μm

TABLE I
GVD AND NONLINEAR COEFFICIENT VALUES OF TBY FIBER WITH DIFFERENT CORE DIAMETERS AT TWO PUMPING WAVELENGTHS

Core diameter(μm)	1.96 μm			2.8 μm		
	β_2 (ps^2/km)	γ (W^{-1}km^{-1})	$\gamma/\lvert\beta_2\rvert$	β_2 (ps^2/km)	γ (W^{-1}km^{-1})	$\gamma/\lvert\beta_2\rvert$
4.0	-113.2	138.1	1.22	-400.0	87.2	0.218
5.0	-46.9	109.8	2.34	-284.1	72.2	0.254
6.0	-29.0	69.6	2.40	-242.5	46.8	0.193
7.0	-24.2	52.7	2.18	-255.4	35.9	0.141

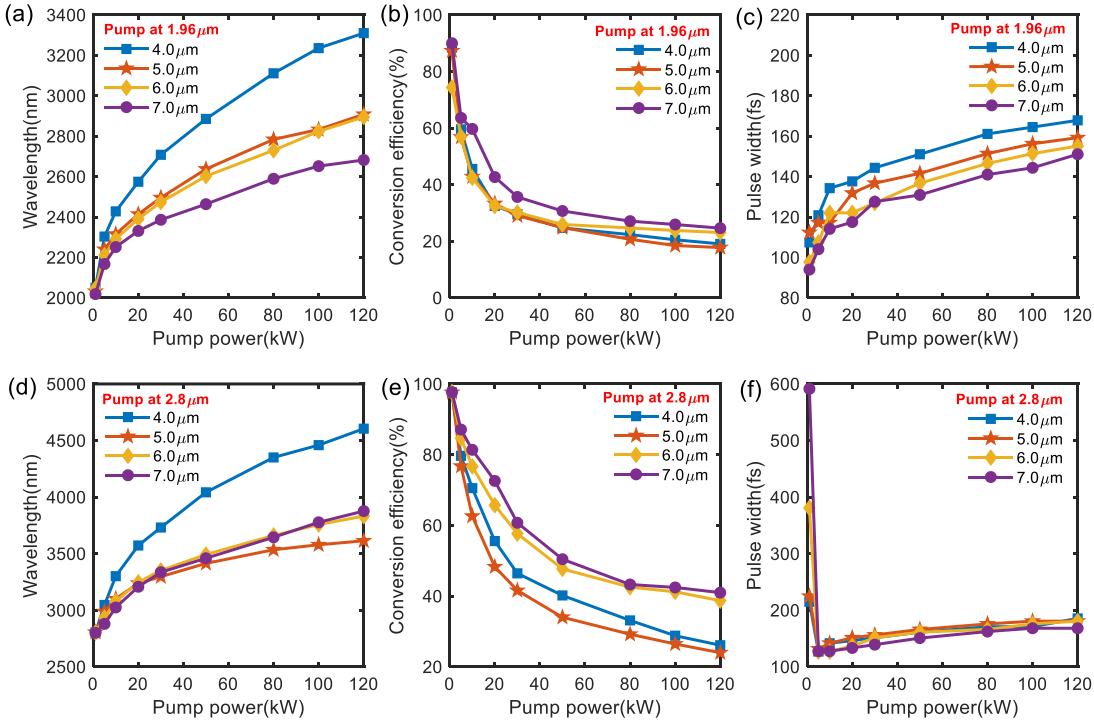

Fig. 5. Comparison of the TBY fiber with core diameters of 4 μm, 5 μm, 6 μm, and 7 μm. (a) the wavelength, (b) conversion efficiency, and (c) pulse width of the most shifted soliton with a 1.96 μm pump. (e) wavelength, (f) conversion efficiency, and (g) pulse width of the most shifted soliton with a 2.8 μm pump.

at the concerning wavelength. The TBY fibers with the chosen core diameters all work in the anomalous dispersion region in the 2-5 μm spectrum region. While the TBY fiber with other core diameters beyond this range does not have this property [15], [25]. One could see that the 4-μm-core fiber has larger $|\beta_2|$ and γ values at both 1.96 μm and 2.8 μm compared with other candidates. With unknown pump energy and duration (i.e., unknown soliton order), the $\gamma/|\beta_2|$ value of the fiber could be a crucial quantity to describe the characteristics of a Raman shifter fiber. As indicated in formula (6), with the same input power and pulse width, the higher the $\gamma/|\beta_2|$ value, the higher the soliton order N. All the four groups have a larger $\gamma/|\beta_2|$ value at 1.96 μm, indicating the generation of a higher-order soliton under the same input power. The 6-μm-core fiber has a $\gamma/|\beta_2|$ value of 2.40 at 1.96 μm, which is the largest among the four candidates. While at 2.8 μm the 5-μm-core fiber has the largest $\gamma/|\beta_2|$ value of 0.254. Therefore, with the same input pulse, they are expected to produce the highest order solitons at the corresponding wavelength.

Fig. 5 displays the calculated wavelength, conversion efficiency, and FWHM pulse width of the most red-shifted Raman soliton using the TBY fiber with a core diameter ranging from 4 μm to 7 μm as the nonlinear medium. The set of the pump peak power is the same as the preceding simulation. Fig. 5(a), (b), and (c) show the characteristics of the most red-shifted soliton with pump pulses at 1.96 μm. As shown in Fig. 5(a), the wavelength of the most red-shifted solitons increases with the decrease of the fiber's core diameter (i.e., increase of nonlinearity). With a pump peak power of 120 kW, the most red-shifted soliton is located at 3310 nm, 2908 nm, 2895 nm, and 2682 nm using the fiber with a core diameter of 4 μm, 5 μm, 6 μm, and 7 μm, respectively. The results in Fig. 5(b) show the conversion efficiency of each case. As the pump power increases, the conversion efficiency in the four groups all decreases. When the pump power reaches 120 kW, the optical conversion efficiency is 19.1%, 17.8%, 23.1% and 24.6% for the core diameter of 4 μm, 5 μm, 6 μm, and 7 μm, respectively. The relatively low soliton order and dispersion help the 7-μm-core fiber hold the highest conversion

efficiency among the four groups. The conversion efficiency in the 5-μm-core fiber and 6-μm-core fiber is limited by a higher soliton order, which greatly confines the energy transference to the first fundamental soliton, resulting in low conversion efficiency. As the soliton shifts to a longer wavelength, the influence of dispersion becomes stronger, which directly transfers the energy of the first soliton to dispersive waves [34]. For the 4-μm and 5-μm-core fiber has the largest dispersion, the conversion efficiency in them gradually lags behind that in the 6-μm-core fiber as the power increases. And this is also the main reason that the wavelength conversion using the 5-μm and 6-μm-core fiber gets closer in high power cases as shown in Fig. 5(a). Fig. 5(c) shows the pulse duration of the four groups. With the increasing pump power, the soliton shifts to a longer wavelength and experiences a large anomalous dispersion, which leads to the temporal broadening of the soliton pulse. With 120 kW pump power, the pulse duration of the most red-shifted soliton is 167 fs, 159 fs, 155 fs, and 151 fs for the four candidates. As displayed in Fig. 4(a) and (b), the duration of the output pulse increases because of increasing $|\beta_2|$ value and decreasing γ and P_0 value. And the results in Fig. 5(c) are in high consistency with this observation, with the output pulse duration increasing with the increase of fiber's core diameter (i.e., increase of dispersion and decrease of nonlinearity).

Fig. 5(d), (e), and (f) display the simulation results using the 2.8-μm-pump. The longest soliton fission length (in the case with 7-μm-core fiber, 5 kW pump power) is calculated as 8.4×10^{-4} cm. Therefore, the 15 cm-long fiber is enough for the soliton evolution. As displayed in Fig. 5(d), the four groups' pattern of wavelength conversion versus pump power is complex. Before 20 kW, it follows the same formula as in Fig. 5(a) that the smaller the core diameter, the larger the wavelength conversion is. At 20 kW, the wavelength of the most red-shifted soliton using the 6-μm-core fiber (3247 nm) exceeds that using the 5-μm-core fiber (3238 nm). A similar scenario occurs with 30 kW pump power, where the soliton wavelength obtained using the 7-μm-core fiber (3336 nm) exceeds that using the 5-μm-core fiber (3297 nm). At 100 kW, the performance of the 7-μm-core fiber (3777 nm) exceeds the 6-μm-core fiber (3757 nm). Although the separate effect of dispersion and nonlinearity on soliton evolution have been determined by previous theoretical works [36], [37], it fails to explain the performance of the TBY fiber with different core diameters in Fig. 5(a) and (d). This is because the candidate with a higher nonlinearity simultaneously has a larger anomalous dispersion. The SSFS rate estimate in adiabatic approximation [14] cannot explain the difference in the SSFS capability of different fibers under different pump power. Qualitatively, we can introduce the effect of the soliton order to interpret this phenomenon. A higher soliton order compresses the pulse in the temporal domain, as indicated in formula (7). Because the soliton splitting duration is inversely proportional to the soliton order, this effect is strong in low power cases but weak in high power cases. On the other hand, the higher soliton order reduces the energy proportion of the first soliton, especially dominating in high-power cases. Consequently, at the same power and pulse shape, a higher soliton order would improve the wavelength conversion in low power cases but weaken this process in high power cases. In this case, for possessing a much higher $\gamma/|\beta_2|$ than the other groups, the 5 μm one performs the worst in wavelength conversion with high-power pump. The 4 μm one both possesses the highest nonlinearity and lowest soliton order, resulting in much better than the other three groups in high-power cases. With 120 kW pump power, the most red-shifted soliton reached 4605 nm with the 4-μm-core fiber, while the wavelength extension in the other three groups is below 4 μm. Fig. 5(e) shows the conversion efficiency curve as the function of pump power, which is qualitatively similar to the scenario with the 1.96 μm pump scheme. And as discussed in the preceding, using a 2.8 μm pump could bring a higher conversion efficiency. When the pump power reaches 120 kW, the conversion efficiency is 26.1%, 24.4%, 34.7%, and 41.0%. The 7 μm maintains the best performer for it has the lowest soliton order and dispersion. Fig. 5(f) displays the pulse duration of the four groups. With 1 kW pump power, the pulse duration is 215 fs, 200 fs, 649 fs, and 591 fs for the four groups, which is much wider than the pump pulse. This is caused by the low $\gamma/|\beta_2|$ value of all groups at 2.8 μm, which fails to support a unit soliton number and leads to the elongation process. As the pump power increases, the pulse duration first decreases due to the soliton fission, then constantly increases as the soliton shifts to a longer wavelength. Eventually, the pulse duration reaches 186 fs, 181 fs, 166 fs, and 168 fs for the four groups. The principle is similar as discussed in the preceding.

V. Measurement of the Frequency Shift Ability of a Raman Shifter Fiber and Ways for Optimization

The above numerical studies revealed the effect of the pumping wavelength on the SSFS performance, and the engineering of the fiber's nonlinearity and dispersion for the optimization of the conversion efficiency and pulse duration of a Raman soliton system. However, as one most important aspect, the improvement of the wavelength conversion through regulating the fiber's nonlinearity and dispersion has not been clarified by previous theory. In the preceding content, we propose a qualitative explanation to this issue based on the different roles of the soliton order in low-power and high-power cases. While a deeper discussion on this issue is necessary, aiming at finding an optimal combination of the fiber's nonlinearity and dispersion for the largest wavelength conversion. A semi-quantitative measurement of the fiber's relative advantage in wavelength conversion as a function of the soliton order N and nonlinear coefficient γ can be made as follow:

$$W_{\text{fiber}} = \begin{cases} c_1\gamma(2N-1)^2 N \le N_c \\ c_2\gamma\left(\frac{2N-1}{N^2}\right)^4 N > N_c \end{cases} \tag{9}$$

where c_1, c_2 are the scaling coefficients, N_c is the critical soliton order and W_{fiber} denotes the relative advantage of the fiber in terms of wavelength conversion under the same pump power and shape.

This formula is derived from the idea that in low-power cases ($N \le N_c$) the main role of a higher soliton order is compressing the pulse in the temporal domain. While in high-power cases ($N > N_c$) the effect of a higher soliton order is mainly lowering

TABLE II
THE SOLITON ORDER OF THE BEST PERFORMER IN EACH TESTED PARAMETER

Wavelength	1.96 μm				2.8 μm			
Parameter	5 kW	10 kW	15 kW	20 kW	5 kW	10 kW	15 kW	20 kW
5 $W^{-1}km^{-1}$	6.48	6.13	5.84	6.89	6.13	6.13	6.13	7.4
10 $W^{-1}km^{-1}$	6.13	6.89	6.47	6.13	6.13	6.47	6.47	5.84
15 $W^{-1}km^{-1}$	6.48	6.48	6.13	6.13	6.13	5.84	6.13	6.13
20 $W^{-1}km^{-1}$	6.89	6.48	5.84	5.84	6.47	6.13	5.84	6.13
25 $W^{-1}km^{-1}$	6.89	5.84	5.84	5.84	6.13	6.13	6.13	6.13
30 $W^{-1}km^{-1}$	6.47	6.13	6.13	6.47	6.13	5.84	6.13	5.84

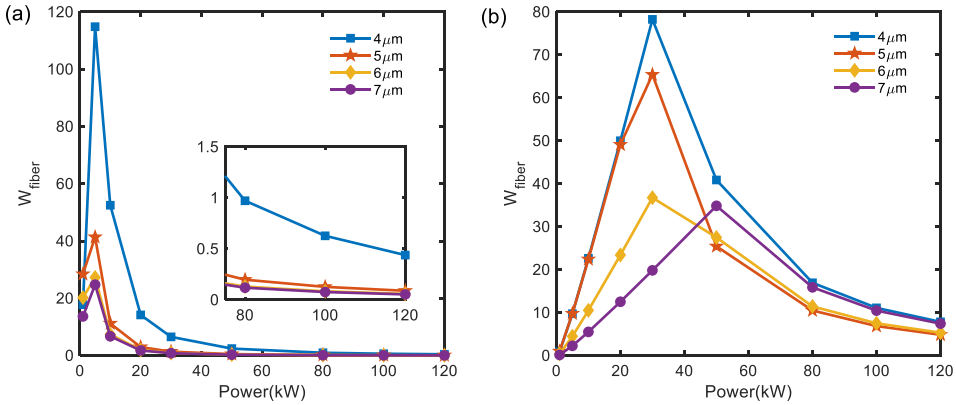

Fig. 6. The calculated W_{fiber} values of the TBY fiber with a core diameter ranging from 4 to 7 μm with (a) 1.96-μm-pump and (b) 2.8-μm-pump.

the energy portion of the first soliton. Concerning the relation that the frequency shift amount is in proportion with $1/T^2$ [28] and ${E_S}^4$ [14] in the adiabatic approximation, formula (9) could be easily derived based on formula (7). From the physical interpretation of GNLSE, we could regard the value of the nonlinear coefficient γ represents the largest wavelength conversion ability of a Raman shifter fiber. To ensure the continuity and normalization of W_{fiber} except the multiplier of γ, the scaling coefficients c_1, c_2 can be written as follow:

$$c_1 = \frac{1}{(2N_c - 1)^2}, c_2 = \left(\frac{N_c^2}{2N_c - 1}\right)^4 \tag{10}$$

Considering that $W_{fiber}(N)$ is increasing when $N < N_c$ and is decreasing when $N > N_c$, N_c is supposed to be an optimal soliton order value for maximizing the wavelength conversion. In Fig. 5(e) the soliton order N changes from 5.1 to 6.3, and 5.5 to 9.0 when the advantages of the 5-μm-core and 6-μm-core fiber over the 7-μm-core decrease. The optimal soliton order could locate in that range. A larger test data is required to obtain this value more rigorously. To do so, the GNLSE is treated as a prototype, neglecting the frequency-dependency, fiber loss, and high order dispersion. With this simplification, the effect of the soliton order can be emphasized. Due to our simplified treatment of dispersion and loss, we consider the value of the nonlinear coefficient and the relatively low value of input energy to ensure reasonable results.

We consider parameters of typical fibers for SSFS, with γ changing from 5, 10, 15, 20, 25, and 30 $W^{-1}km^{-1}$, pump peak power changing from 5, 10, 15, and 20 kW. For each γ value, 20 β_2 values are used to generate solitons with a soliton order from 4 to 10. In this case, 20 kinds of Raman shifter fiber are formulated for each γ-power combination. The soliton order of the best performer is selected and shown in Table II. One can see that for each tested parameter, the soliton order of the best performer is all $\sim$6. The average soliton order with pumping wavelength at 1.96 and 2.8 μm is 6.29 and 6.17 respectively. The N_c value is taken as the total average of 6.23 and substituted to (9) to interpret the results in Fig. 5.

The results in Fig. 6(a) and (b) display the W_{fiber} values of the four candidates with 1.96-μm-pump and 2.8-μm-pump, respectively. As shown in Fig. 6(a), except the first case, the W_{fiber} values decrease with the fiber's core diameter, which is in good agreement with the results in Fig. 5(a) that the wavelength conversion decreases with the fiber's core diameter. Before 10 kW, the W_{fiber} value increases with the pump power as the soliton order approaches N_c. After 10 kW, the W_{fiber} value decreases with the pump power for it penalizes the soliton order larger than N_c. The results in Fig. 6(b) explicitly predicts the scenario that the 6-μm-core fiber exceeds the 5-μm-core fiber, and the 7-μm-core fiber exceeds the 5-μm-core and 6-μm-core fiber. The predicted critical pump power when the 6-μm-core fiber exceeds the 5-μm-core fiber is higher than the practical case shown in Fig. 5(e). This is because the 5-μm-core fiber has larger higher-order dispersions, transferring more energy of the first soliton, and accelerating the process of its lagging behind. Due to a similar reason, the prediction of the 7-μm-core fiber is forward

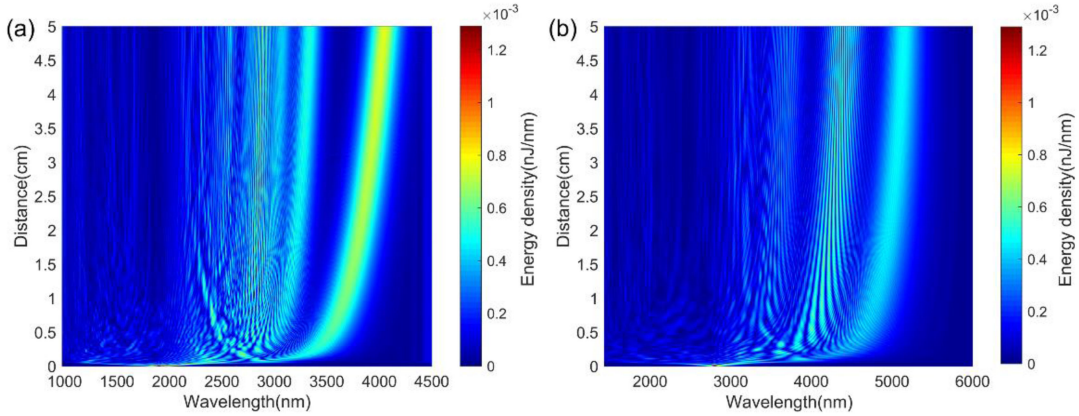

Fig. 7. The calculated spectrum evolution versus propagation distance when (a) pumping at 1.9 μm using the source in [12] and (b) pumping at 2.8 μm using the source in [21].

than the practical case for it has a larger higher-order dispersion than the 5-μm-core and 6-μm-core fiber. Simultaneously, the wavelength-dependent fiber loss distorted the prediction results. Despite these perturbations, this model still offers a good measurement for the frequency shift ability of Raman shifter fiber.

These results involving the comparison of two typical pumping schemes and TBY fiber with different core diameters reveal some feasible ways to optimize the performance of all Raman soliton sources: 1. To achieve the largest wavelength extension, the nonlinearity of the Raman shifter fiber should be as high as possible under the premise that the soliton order is moderate (i.e., a higher W_{fiber} value). The fiber length should be as long as possible. 2. To achieve high conversion efficiency and short pulse duration, one should manage to control the SSFS process in a soliton order as low as possible ($>$1) and choose a Raman shifter fiber with low dispersion (especially higher-order dispersion) in the operation spectrum. Use a $\sim$2.8-μm-pump and the fiber length should be as short as possible. 3. To improve the spectrum cleanliness, the soliton order should be as low as possible ($>$1). Use a $\sim$2.8-μm-pump and the fiber length should be as short as possible. It is noted that the trade-off of the three concerning aspects is usually inherent.

VI. Further Wavelength Extension by Cascading the TBY Fiber With Chalcogenide Fiber

The discussions in the preceding have demonstrated that the TBY fiber is a good nonlinear medium for the SSFS process. However, as displayed in Fig. 1(c), the loss of the TBY fiber increases steeply as the wavelength approaches 5 μm, confining the further wavelength extension. In our previous work [37], we have demonstrated that the cascaded SSFS structure is a feasible way to further extend the soliton wavelength. This could also be a feasible way to overcome the obstacle brought by the loss spectrum of the TBY fiber. Many chalcogenide fibers possess low fiber loss in the spectrum range beyond 5 μm. However, the ZDW of these chalcogenide fibers is usually beyond 3.5 μm, manifesting that it demands a pumping wavelength larger than 3.5 μm to excite the SSFS effect. However, mode-locked pump source with such demand has not been achieved yet. As demonstrated in the preceding, using a 2-μm or 2.8-μm-pump, the TBY fiber can offer a wavelength extension larger than the ZDW of the chalcogenide fibers. Therefore, cascading the TBY fiber with a chalcogenide fiber could be a feasible way to achieve better SSFS performance.

To demonstrate the potential of this cascading SSFS structure, we used the TBY fiber with a core diameter of 4 μm as the first stage Raman shifter. The experimentally achievable high power, short duration mode-locked pulses at $\sim$2 μm [12] and $\sim$2.8 μm [22] were used as the seed pulse. Inspired by the results in Fig. 4, the length of the TBY fiber is optimized to 5 cm, which is long enough for expected wavelength conversion and simultaneously preserves energy and short duration for the SSFS process in the following chalcogenide fiber. Fig. 7(a) displays simulation results of launching the 40 nJ, 117 fs (FWHM) seed pulse at 1.9 μm to the TBY fiber. The 1.9-4.1 μm wavelength conversion was achieved, with an output energy of 6 nJ and FWHM pulse width of 96 fs at 4.1 μm. Fig. 7(b) displays the scenario of using the 2.8 μm seed pulse with a pulse width of 137 fs (FWHM) and energy of 30 nJ. The results are impressive, with the most red-shifted soliton reaching 5.2 μm. At 5.2 μm, the most red-shifted has an energy of 5.2 nJ and a pulse duration of 112 fs.

The $AsSe_2$-As_2S_5 fiber [40] was employed as the next stage Raman shifter fiber. It has a higher nonlinearity than the TBY fiber at the coupling wavelength and possesses a wide anomalous dispersion region beyond 4 μm. Moreover, it possesses low loss in the 4-9 μm spectrum range. The coupling efficiency between the TBY fiber and the $AsSe_2$-As_2S_5 fiber was calculated as [9]:

$$\eta = \frac{E_{in}}{E_o} = \frac{4\left(A_{eff}^{TBY} A_{eff}^{AsSe_2-As_2S_5}\right)}{\left(A_{eff}^{TBY} + A_{eff}^{AsSe_2-As_2S_5}\right)^2} \tag{11}$$

where η denotes the coupling efficiency, *Eo* is the output energy of the TBY fiber, E_{in} is the energy coupled into the $AsSe_2$-As_2S_5 fiber, A_{eff}^{TBY}, and $A_{eff}^{AsSe2\text{-}As2S5}$ are mode effective areas of two

TABLE III
GVD, NONLINEAR COEFFICIENT, AND MODE EFFECTIVE AREA VALUES OF $AsSe_2$-As_2S_5 FIBER WITH CORE DIAMETERS RANGING FROM 4.5 TO 6.5 μm AT 4.1 μm AND 5.2 μm

Core diameter(μm)	4.1 μm			5.2 μm		
	β_2 (ps^2/km)	γ (W^{-1}km^{-1})	A_{eff}(μm^2)	β_2 (ps^2/km)	γ (W^{-1}km^{-1})	A_{eff}(μm^2)
4.5	-248.3	531.2	9.2	-657.4	234.0	10.2
5.0	-181.7	459.0	11.0	-586.5	195.7	12.0
5.5	-116.8	389.2	13.0	-504.3	172.1	14.0
6.0	-66.0	333.9	15.1	-432.6	145.0	16.1
6.5	-22.6	289.4	17.5	-367.2	126.5	18.5

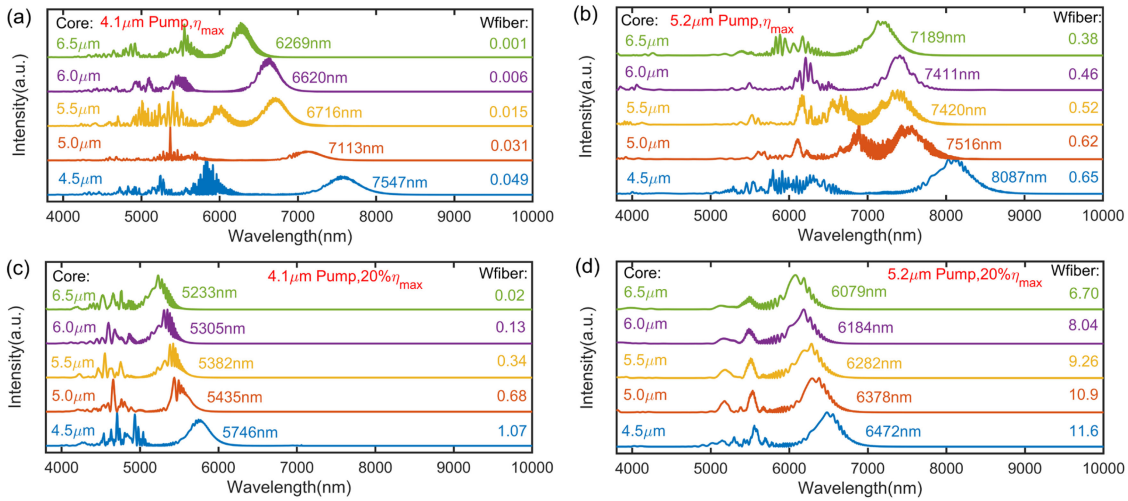

Fig. 8. The calculated output spectra of the 10 cm-long $AsSe_2$-As_2S_5 fiber with a core diameter ranging from 4.5 μm to 6.5 μm. (a) use the 4.1 μm pump, (b) use the 5.2 μm pump generated from the TBY fiber when considering the maximum coupling efficiency. (c) use the 4.1 μm pump, (b) use the 5.2 μm pump generated from the TBY fiber when considering 20% of the maximum coupling efficiency.

fibers. The A_{eff}^{TBY} value is 9.8 μm^2 and 12.3 μm^2 at 4.1 μm and 5.2 μm, respectively.

Table III shows the calculated β_2, γ, and A_{eff} values of the $AsSe_2$-As_2S_5 fiber with core diameters ranging from 4.5 to 6.5 μm, using the refractive index data in [40]. The nonlinear refractive index is estimated as $n_2 = 9.3 \times 10^{-19}$ m^{2}W^{-1} at 4.1 μm and $n_2 = 5.5 \times 10^{-19}$ m^{2}W^{-1} at 5.2 μm based on data in [17], [40]. The $AsSe_2$-As_2S_5 fiber with the core diameters we choose has high coupling efficiency (>92%), which preserves the soliton energy. The nonlinearity and dispersion of these $AsSe_2$-As_2S_5 fibers ensure a suitable soliton matching condition [41]. The $AsSe_2$-As_2S_5 fiber with a core diameter beyond the range of 4.5-6.5 μm may have a positive β_2 value in the spectrum that the shifted Raman soliton may cover, which fails to support the SSFS process. The length of the $AsSe_2$-As_2S_5 fiber is taken as 10 cm, which is long enough for the soliton evolution. The Raman response parameter in $AsSe_2$-As_2S_5 fiber is $f_R = 0.148$, $\tau_1 = 15.34$ fs and $\tau_2 = 106.1$ fs [40].

The calculated output spectra from the 10 cm-long $AsSe_2$-As_2S_5 fiber with the core diameter ranging from 4.5 to 6.5 μm is shown in Fig. 8. The results in Fig. 8(a) and (b) consider the maximum coupling efficiency as calculated in (11). As shown in Fig. 8(a), when a 4.1-μm-pump was used, the $AsSe_2$-As_2S_5 fiber with a core diameter of 4.5 μm allows SSFS process up to 7547 nm. At 7547 nm, the most red-shifted Raman soliton has an energy of 1.5 nJ with a pulse width of 150 fs. The frequency shift ability of each Raman shifter fiber is in high accordance with the W_{fiber} value. Fig. 8(b) displays the scenario using a 5.2-μm pump pulse. An impressive wavelength extension up to 8087 nm was achieved using the 4.5-μm-core fiber. The most red-shifted Raman soliton at 8087 nm has an energy of 2.0 nJ and a duration of 138 fs. Considering that the practical coupling efficiency could not be as high as calculated by formula (11), the performance of the $AsSe_2$-As_2S_5 fiber in low coupling efficiency should be examined. The results considering 20% of the maximum coupling efficiency are shown in Fig. 8(c) and (d). It can be seen that the $AsSe_2$-As_2S_5 fiber still offers a considerable wavelength extension even with such a poor coupling efficiency. As shown in Fig. 8(a), when the coupling wavelength is set at 4.1 μm, the 4.5-μm-core $AsSe_2$-As_2S_5 fiber extends the soliton wavelength to 5746 nm. When using the 5.2 μm seed pulse obtained from the TBY fiber, the 4.5-μm-core fiber extends the soliton wavelength to 6472 nm. The 4.5-μm-core fiber has the highest W_{fiber} value and is the best performer among the five candidates, meaning

that it has the best coordination of nonlinearity and dispersion. The W_{fiber} value of the other four candidates is also in high consistency with the wavelength conversion, which verifies that the W_{fiber} value we proposed is an effective quantity to find the best Raman shifter fiber. Particularly, W_{fiber} is a good index to compare the frequency shift ability of different Raman shifters fiber when the same pump is used. The comparison of the W_{fiber} value under different pumps is meaningless. Noting that in this calculation we used the experimentally achievable seed pulse and considered poor coupling condition, the cascading of the TBY fiber and $AsSe_2$-As_2S_5 fiber could be a quite feasible way to achieve SSFS performance better than current level.

VII. Conclusion

We have numerically studied the SSFS process in the TBY fiber. First, we study the impacts of the pumping wavelength ($\sim$2 μm and $\sim$2.8 μm) on the SSFS process in the TBY fiber. Numerical results show that with the same input energy and pulse shape, using a 1.96-μm pumping scheme could lead to larger frequency conversion and a shorter pulse duration than the 2.8-μm pumping scheme. While the 2.8-μm pumping scheme could improve the spectrum cleanliness and conversion efficiency of the Raman soliton. A centimeter-scale length is proved to be enough for the TBY fiber to achieve the most wavelength conversion through the SSFS effect. Among the TBY fibers working in the anomalous dispersion region in MIR, with the same pump pulses, the 4-μm-core fiber could achieve the largest wavelength conversion, and the 7-μm-core fiber could generate Raman solitons with the highest conversion efficiency and shortest pulse duration.

As an interpretation of the complex SSFS behavior of TBY fibers, we derive a new quantity W_{fiber} to compare the frequency shift ability of different Raman shifter fibers, which offers a good explanation for the simulation results. Based on these discussions, we have provided general ways to optimize the Raman soliton source: 1. To improve the wavelength conversion: higher nonlinearity under the premise of a moderate soliton order (i.e., a higher W_{fiber} value) and a longer fiber length. 2. To improve conversion efficiency and achieve shorter pulse duration: lower soliton order ($>$1), lower dispersion in the operating spectrum, and shorter fiber length. Use pump pulse at $\sim$2.8 μm. 3. To improve the spectrum cleanliness: lower soliton order ($>$1). Use pump pulse at $\sim$2.8 μm.

Using the experimentally achievable seed pulse source at 1.9 and 2.8 μm, we demonstrate a widely tunable Raman soliton laser in TBY fiber covering the spectrum range of 1.9-4.1 μm and 2.8-5.2 μm. We propose the idea of cascading the TBY fiber with the $AsSe_2$-As_2S_5 fiber and demonstrated the possibility of wavelength extension up to 8087 nm through the SSFS process. Even with poor coupling efficiency, the cascading of the $AsSe_2$-As_2S_5 fiber still offers a considerable wavelength extension. The W_{fiber} value we proposed is in high consistency with the simulation results of the $AsSe_2$-As_2S_5 fiber, which could offer meaningful guidance for choosing a good Raman shifter fiber.

References

[1] F. K. Tittel, D. Richter, and A. Fried, "Mid-infrared laser applications in spectroscopy," *Top. Appl. Phys.*, vol. 89, pp. 458–529, 2003.

[2] M. R. McCurdy, Y. Bakhirkin, G. Wysocki, R. Lewicki, and F. K. Tittel, "Recent advances of laser-spectroscopy-based techniques for applications in breath analysis," *J. Breath Res.*, vol. 1, no. 1, 2007, Art. no. 014001.

[3] I. T. Sorokina, V. V. Dvoyrin, N. Tolstik, and E. Sorokin, "Mid-IR ultrashort pulsed fiber-based lasers," *IEEE J. Sel. Topics Quantum Electron.*, vol. 20, no. 5, Sep./Oct. 2014, Art. no. 0903412.

[4] P. Agostini and L. F. Dimauro, "The physics of attosecond light pulses," *Rep. Prog. Phys.*, vol. 67, no. 6, pp. 813–855, 2004.

[5] F. M. Mitschke and L. F. Mollenauer, "Discovery of the soliton self-frequency shift," *Opt. Lett.*, vol. 11, no. 10, pp. 659–661, 1986.

[6] P. Wang, H. Shi, F. Tan, and P. Wang, "Enhanced tunable Raman soliton source between 1.9 and 2.36 μm in a Tm-doped fiber amplifier," *Opt. Exp.*, vol. 25, no. 14, pp. 16643–16651, 2017.

[7] F. Liu *et al.*, "Study on soliton self-frequency shift in a Tm-doped fiber amplifier seeded by a Kelly-sideband-suppressed conventional soliton," *Opt. Exp.*, vol. 29, no. 5, pp. 6553–6562, 2021.

[8] E. A. Anashkina, A. V. Andrianov, M. Y. Koptev, V. M. Mashinsky, and A. V. Kim, "Generating tunable optical pulses over the ultrabroad range of 1.6–2.5 μm in geO_2-doped silica fibers with an Er:Fiber laser source," *Opt. Exp.*, vol. 20, no. 24, pp. 27102–27107, 2012.

[9] E. A. Anashkina, A. V. Andrianov, M. Yu. Koptev, S. V. Muravyev, and A. V. Kim, "Generating femtosecond optical pulses tunable from 2 to 3 μm with a silica-based all-fiber laser system," *Opt. Lett.*, vol. 39, no. 10, pp. 2963–2966, 2014.

[10] T. Du *et al.*, "2.01$\sim$2.42 μm all-fiber femtosecond Raman soliton generation in a heavily germanium doped fiber," *IEEE J. Sel. Topics Quantum Electron.*, vol. 25, no. 4, Jul./Aug. 2019, Art. no. 1400207.

[11] S. Duval *et al.*, "Watt-level fiber-based femtosecond laser source tunable from 2.8 to 3.6 μm," *Opt. Lett.*, vol. 41, no. 22, pp. 5294–5297, 2016.

[12] Y. Tang, L. G. Wright, K. Charan, T. Wang, C. Xu, and F. W. Wise, "Generation of intense 100 fs solitons tunable from 2 to 4.3 μm in fluoride fiber," *Optica*, vol. 3, no. 9, pp. 948–951, 2016.

[13] M. Y. Koptev *et al.*, "Widely tunable mid-infrared fiber laser source based on soliton self-frequency shift in microstructured tellurite fiber," *Opt. Lett.*, vol. 40, no. 17, pp. 4094–4097, 2015.

[14] E. A. Anashkina, A. V. Andrianov, V. V. Dorofeev, and A. V. Kim, "Toward a mid-infrared femtosecond laser system with suspended-core tungstate-tellurite glass fibers," *Appl. Opt.*, vol. 55, no. 17, pp. 4522–4530, 2016.

[15] Z. Li *et al.*, "Tunable mid-infrared raman soliton generation from 1.96 to 2.82 μm in an all-solid fluorotellurite fiber," *AIP Adv.*, vol. 8, no. 11, 2018, Art. no. 115001.

[16] A. C. Judge, S. A. Dekker, R. Pant, C. Sterke, and B. J. Eggleton, "Soliton self-frequency shift performance in As_2S_3 waveguides," *Opt. Exp.*, vol. 18, no. 14, pp. 14960–14968, 2010.

[17] F. Wang *et al.*, "Numerical demonstration of widely tunable femtosecond soliton generation in chalcogenide microstructured fibers," *Laser Phys. Lett.*, vol. 16, no. 10, 2019, Art. no. 105402.

[18] I. Alamgir, M. Shamim, W. Correr, Y. Messaddeq, and M. Rochette, "Mid-infrared soliton self-frequency shift in chalcogenide glass," *Opt. Lett.*, vol. 46, no. 21, pp. 5513–5516, 2021.

[19] J. Luo, B. Sun, J. Ji, E. L. Tan, and Y. Xia, "High-efficiency femtosecond raman soliton generation with a tunable wavelength beyond 2 μm," *Opt. Lett.*, vol. 42, no. 8, pp. 1568–1571, 2017.

[20] P. Wang, C. Bao, B. Fu, X. Xiao, P. Grelu, and C. Yang, "Generation of wavelength-tunable soliton molecules in a 2-μm ultrafast all-fiber laser based on nonlinear polarization evolution," *Opt. Lett.*, vol. 41, no. 10, pp. 2254–2257, 2016.

[21] J. Li, D. D. Hudson, Y. Liu, and S. D. Jackson, "Efficient 2.87 μm fiber laser passively switched using a semiconductor saturable absorber mirror," *Opt. Lett.*, vol. 37, no. 18, pp. 3747–3749, 2012.

[22] J. Huang *et al.*, "Sub-two-cycle octave-spanning mid-infrared fiber laser," *Optica*, vol. 7, no. 6, pp. 574–579, 2020.

[23] G. Tao *et al.*, "Infrared fibers," *Adv. Opt. Photon.*, vol. 7, no. 2, pp. 379–458, 2015.

[24] C. Yao *et al.*, "Holmium-doped fluorotellurite microstructured fibers for 2.1 μm lasing," *Opt. Lett.*, vol. 40, no. 20, pp. 4695–4698, 2015.

[25] C. Yao *et al.*, "High-power mid-infrared supercontinuum laser source using fluorotellurite fiber," *Optica*, vol. 5, no. 10, pp. 1264–1270, 2018.

[26] J. P. Gordon, "Theory of the soliton self-frequency shift," *Opt. Lett.*, vol. 11, no. 10, pp. 662–664, 1986.

[27] Y. Kodama and A. Hasegawa, "Nonlinear pulse propagation in a monomode dielectric guide," *IEEE J. Quantum Electron.*, vol. 23, no. 5, pp. 510–524, May 1987.
[28] K. J. Blow and D. Wood, "Theoretical description of transient stimulated raman scattering in optical fibers," *IEEE J. Quantum Electron.*, vol. 25, no. 12, pp. 2665–2673, Dec. 1989.
[29] P. V. Mamyshev and S. V. Chernikov, "Ultrashort-pulse propagation in optical fibers," *Opt. Lett.*, vol. 15, no. 19, pp. 1076–1078, 1990.
[30] P. L. François, "Nonlinear propagation of ultrashort pulses in optical fibers: Total field formulation in the frequency domain," *J. Opt. Soc. Amer. B*, vol. 8, no. 2, pp. 276–293, 1991.
[31] N. Karasawa *et al.*, "Comparison between theory and experiment of nonlinear propagation for a-few-cycle and ultrabroadband optical pulses in a fusedsilica fiber," *IEEE J. Quantum Electron.*, vol. 37, no. 3, pp. 398–404, Mar. 2001.
[32] B. Kibler, J. M. Dudley, and S. Coen, "Supercontinuum generation and nonlinear pulse propagation in photonic crystal fiber: Influence of the frequency-dependent effective mode area," *Appl. Phys. B*, vol. 81, no. 2, pp. 337–342, 2005.
[33] X. Guo *et al.*, "A shower of mid-infrared raman solitons at designed wavelength of $\sim$3 μm from a tapered fluorotellurite fiber," *Laser Phys. Lett.*, vol. 31, no. 9, 2021, Art. no. 09513.
[34] J. M. Dudley, G. Genty, and S. Coen, "Supercontinuum generation in photonic crystal fiber," *Rev. Mod. Phys.*, vol. 78, no. 4, pp. 1135–1184, 2006.
[35] A. A. Rieznik, A. M. Heidt, P. G. König, V. A. Bettachini, and D. F. Grosz, "Optimum integration procedures for supercontinuum simulation," *IEEE Photon. J.*, vol. 4, no. 2, pp. 552–560, Apr. 2012.
[36] M. E. Masip, A. A. Rieznik, P. G. König, D. F. Grosz, A. V. Bragas, and O. E. Martinez, "Femtosecond soliton source with fast and broad spectral tunability," *Opt. Lett.*, vol. 34, no. 6, pp. 842–844, 2009.
[37] D. Kong, D. Jia, D. Feng, C. Ge, Z. Wang, and T. Yang, "Numerical simulation and experimental studies on soliton self-frequency shift in single-mode optical fiber," *Proc. SPIE*, vol. 10825, 2014, Art. no. 1082511.
[38] B. Barviau, O. Vanvincq, A. Mussot, Y. Quiquempois, G. Mélin, and A. Kudlinski, "Enhanced soliton self-frequency shift and CW supercontinuum generation in GeO_2-doped core photonic crystal fibers," *J. Opt. Soc. Amer. B*, vol. 28, no. 5, pp. 1152–1160, 2011.
[39] Y. Hou *et al.*, "Theoretical investigation of a multistage cascaded fiber raman soliton frequency shift system in mid-infrared region," *IEEE Photon. J.*, vol. 13, no. 4, Aug. 2021, Art. no. 1501108.
[40] M. Diouf, A. Wague, and M. Zghal, "Numerical investigation of an ultra-broadband coherent mid-infrared supercontinuum in a chalcogenide $AsSe_2$-As_2S_5 multimaterial photonic crystal fiber," *J. Opt. Soc. Amer. B*, vol. 36, no. 2, pp. 8–14, 2019.
[41] C. Agger, S. T. Sørensen, C. L. Thomsen, S. R. Keiding, and O. Bang, "Nonlinear soliton matching between optical fibers," *Opt. Lett.*, vol. 36, no. 13, pp. 2596–2598, 2011.